(c) Result of laboratory work

[Chemical assay]

Descriptive statistics of elements and factor loading calculated by a principal component analysis is summarized in Appendix I of the Interim Report. In the second factor of the factor matrix, Ag, Fe, Ge and Sb are extracted as elements showing strong positive correlation with Au. Geochemical anomaly map (Fig.4.3.3) represents gold, antimony and tungsten anomalies (>1 ppm Au, > 1 ppm Sb, >100 ppm W).

Maximum gold assay shows 13.1 ppm. Gold anomalies over 1 ppm are recognized at nine samples. These locations make up an alteration zone of silicification and nontronite in north and central part of the sector.

Maximum tungsten assay shows 1,060 ppm. Tungsten anomalies over 100 ppm are recognized at 38 samples. These locations coincide with the alteration zone of silicification and nontronite in northern marginal part in this sector.

In the white argillization zone in the western marginal part of this sector, clay minerals are identified, such as dickite, kaolinite and smectite (Appendix I-2.4).

Clastic deformation is observed under the microscope in siliceous lamina or block parts in the magnetite layer, which has undergone alteration.

[Fluid inclusion test]

Fluid inclusions are observed in quartz crystal of silicification and quartz network in magnetite layer. Fluid inclusions are represented by polyphase, gaseous and liquid inclusions. The polyphase inclusions containing halite crystals can be divided into two groups according to the homogenization temperature. The first group reveals homogenization temperature between 250 and 290°C and salinity ranging from 34 to 37wt% NaCl eq. The second group shows lower homogenization temperature and lower salinity. Its homogenization temperature ranges between 120 and 190°C and its salinity ranges from 28 to 30wt% NaCl eq. (Appendix I in the Interim Report). The silicified magnetite-bearing BIF belonging to the first group is located in the geochemical tungsten anomaly, while silicified magnetite-bearing BIF in the second group is close to the gold anomaly.

[Dating]

Dating has been implemented using amphibole and whole rock sample of meta-amphibolite collected from Ndaouas Mountain, elevation 200m asl, located 17km northeast of the Piment sector. K-Ar dating shows 3190 ± 80Ma and 3080 ± 80Ma, respectively (Appendix I-2.6). It corresponds to Swazian of Archean era. Its age suggests the termination of metamorphism.

K-Ar dating of muscovite samples from pegmatites show almost identical values in 2 samples except one sample observed potassium dissolution (Appendix I-2.6). Within an error, both datings overlap in a range of 2919 - 2909Ma. If the true age of the observed potassium dissolution in

the sample was 2914 Ma (i.e. median of above ages), it would obtain 29 % older age by potassium dissolution.

K-Ar dating of 2 granodiorite samples shows almost similar values (Appendix I-2.6). Within the error, the dating overlaps in a range of 2207 - 2189Ma. These ages are younger than the K-Ar dating values of the above pegmatites. It indicates that there are at least two neutral-acidic igneous activities.

K-Ar dating values of muscovite schist and amphibolite show almost the same age (Appendix I-2.6). Within the error, the dating overlaps in a range of 1733 - 1710Ma. It is assumed that the metamorphism was terminated at this stage.

(d) Consideration

Dating of zircon in gneiss from the Khefissat located in 40 km northwest of the Piment sector has recorded 2900 Ma and 3000 Ma, and zircon in granodiorite from Khefissat has revealed age of 2700 Ma and 2900 Ma (Charendon, 1997).

By the naked eye, no mineralization is recognized in the muscovite schist representing K-Ar dating of 1.7 Ga. Thus, mineralization occurred after 1.7 Ga at the earliest meaning that mineralization took place after Proterozoic.

Owing to the relation with the host rock, the structure geology and alteration, characteristics of mineralization in the Tasiast deposit are considered as listed below:

- Sulfide mineral composed of pyrrhotite occur in disseminated and veinlet forms in magnetite layer of BIF
- Gold mineralization exists with pyrrhotite in and around the rocks showing high metamorphose facies formed garnet.
- Gold mineralization is confirmed along the bedding, fissures and fractures in the magnetite layers.
- Gold mineralization is accompanied by silicification and argillization
- Supergene at the surface makes nontronite, hematite and goethite, and these minerals are mainly recognized at the shallow part of the banded magnetite formation as veinlets and dissemination.
- BIF was formed during Archean about 3.0 Ga, and mineralization took place later than Proterozoic of 1.7 Ga.
- Homogenization temperature of the ore fluid probably related to the gold mineralization ranges from 120 to 190 ° C, and salinity ranges between 28 and 30wt% NaCl eq.

[Remote sensing analysis]

The LANDSAT image including the Tasiast and Tijirit areas, and ASTER images of the Tasiast area are shown in Fig 4.3.9. The conclusions from the image analysis are as follows:

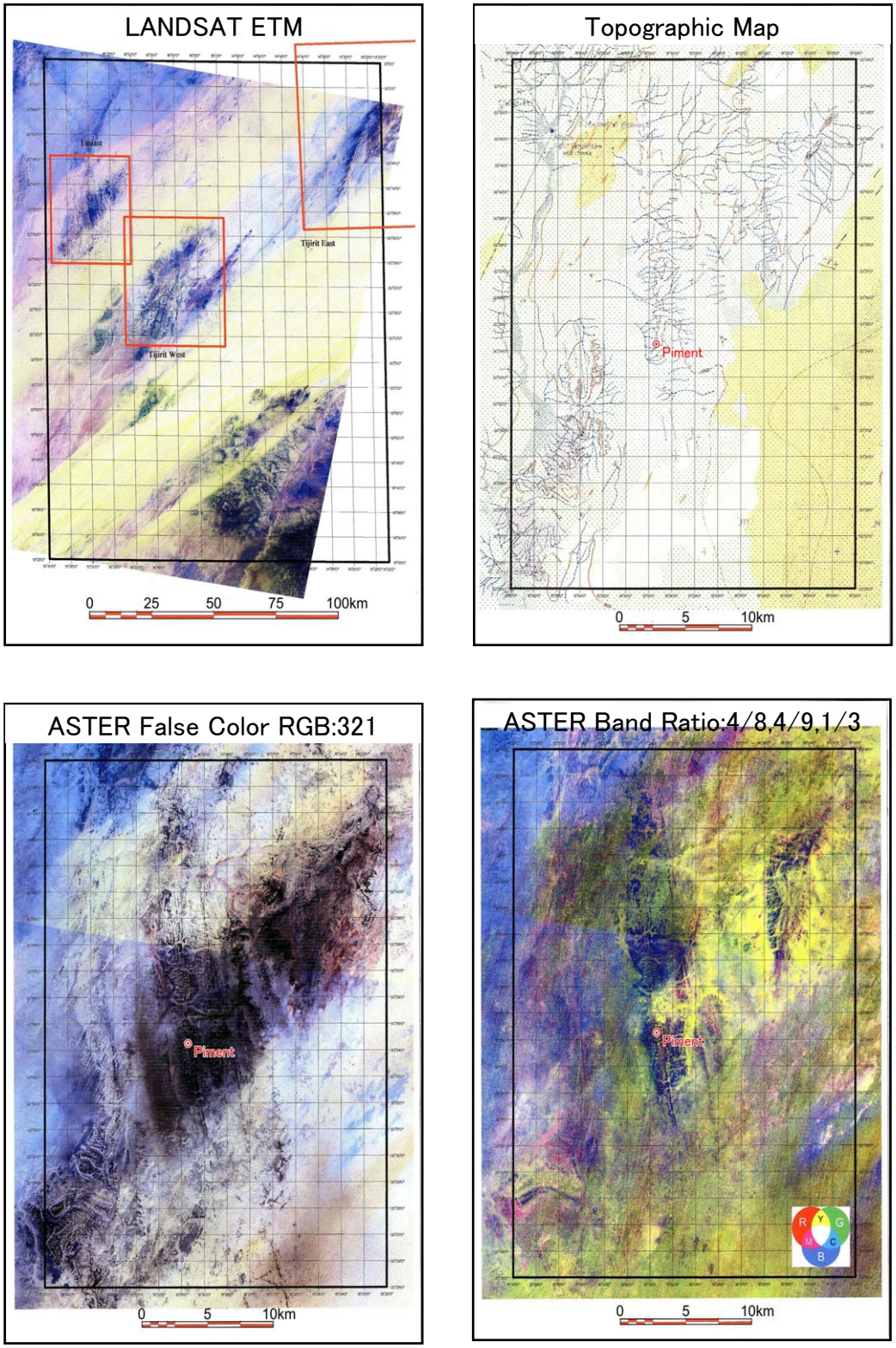

Fig. 4.3.9 Satellite image of the Tasiast and Tijirit areas

- The greenstone belt including BIF is distinguished in dark blue, corresponding to iron oxide in the ASTER Band Ratio image (RGB: 4/8, 4/9, 1/3). Image processing is effective for BIF there.
- The alteration zone accompanied with gold in the Piment sector is not extracted in red (mice), green (clay minerals) and yellow (mica and clay minerals) in ASTER Band Ratio image.
- The dune sediment separating the Tasiast area from the Tijirit area reveals yellowish green and yellow. It is caused by jarosite composing the dune.

It is concluded that it is possible to distinguish BIF in desert region as the Tasiast area by means of the band rationing process.

(4) Tijirit

The Tijirit area is geographically separated from the Tasiast area by the Azefal dune which is situated northwestward of the Tijirit and trends NE-SW with about 20km width (Fig. 4.3.2). However, the southwestern part of the Tijirit comprises the same geological unit as the Tasiast area and consists of tonalite-granodiorite zone, granite-gneiss zone composed of migmatitic gneiss and granodioritic migmatite, and the greenstone belt composed of quartzite, mafic schist, banded iron formation, peridotite, serpentinite and amphibolite.

The Ator sector in the Tijirit area investigated by this survey consists of basic volcanics, amphibolite, serpentinite and schists of probably Archean (PRISM, 2004), but banded iron formation is not found. Compared to the Tasiast area, the NNE-SSW directed structure is distinct and develops dykes and shear zone showing the same direction. Based on lineament extraction on LANDSAT image of the Tijirit area (Fig. 4.3.10), the NNE-SSW lineament is predominant, while the ENE-SWS trend is less dominant. Thus, compression orogenesis has taken place in NE-SE direction.

The deposit in the Ator sector consists of gold-bearing quartz veins existing along a fissure belt in basalt and ophicalcite. The Ator, the principal vein, strikes N20 ° E and dips 70 ° northwest with the maximal thickness of 1m and extension of about 30m. Owing to Schmidt net analyses, the average direction of quartz veins and shear planes reveals a N10 ° E strike and a 74 ° E dip (Fig.4.3.11).

Quartz vein consists of white quartz aggregates less than 1mm in grain size, with a few amount of chlorite. The ore minerals are composed of malachite, hematite and goethite. At the vein with malachite, native gold is often observed by the naked eye. This survey has confirmed that the high grade ore of maximum gold grade of 15.0 g/t and copper grade of 1,820 ppm is recognized (Appendix I-2.5).

Fluid inclusion in quartz veins ranges from 3 to 10 micrometer in size and is dominant in

gaseous inclusions with liquid inclusions and polyphase inclusions containing halite crystals. It is difficult to measure the temperature, because the liquid in many inclusions leaks before gas phase disappears. The quartz vein having 15 g/t for gold assay shows 384°C as homogenization temperature and 45wt% NaCl eq. of salinity (Appendix I of the Interim Report).

K-Ar dating of hornblende in basalt located about 300m south of the Ator vein, shows 2128±75Ma (Appendix I-2.6). It corresponds to the Animikian period of the Proterozoic era. Geological time in this region appeared to be the Archean era based on previous data (PRISM, 2004), however the present survey has confirmed the geological time to be the Proterozoic era

Thus the Tijirit deposit is the vein-type deposit formed in the greenstone belt of the Proterozoic. Fractures trending NNE-SSW have developed by regional metamorphism and deformation caused by orogeny. Along these fractures, highly saline hydrothermal fluid has ascended and formed gold-bearing quartz veins.

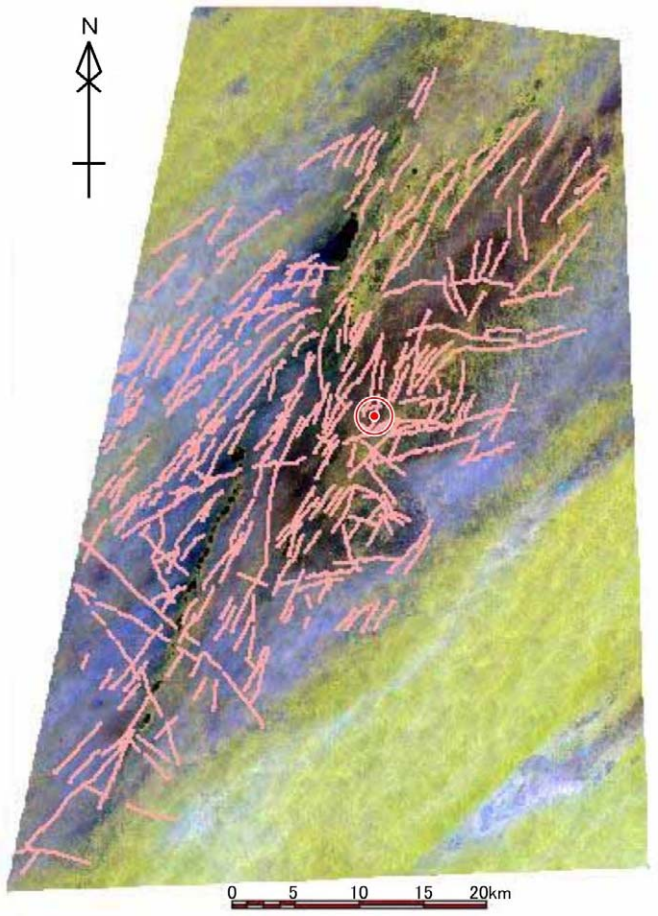

Fig. 4.3 10 Lineament of the Tijirit area
Red circle: Ator gold vein

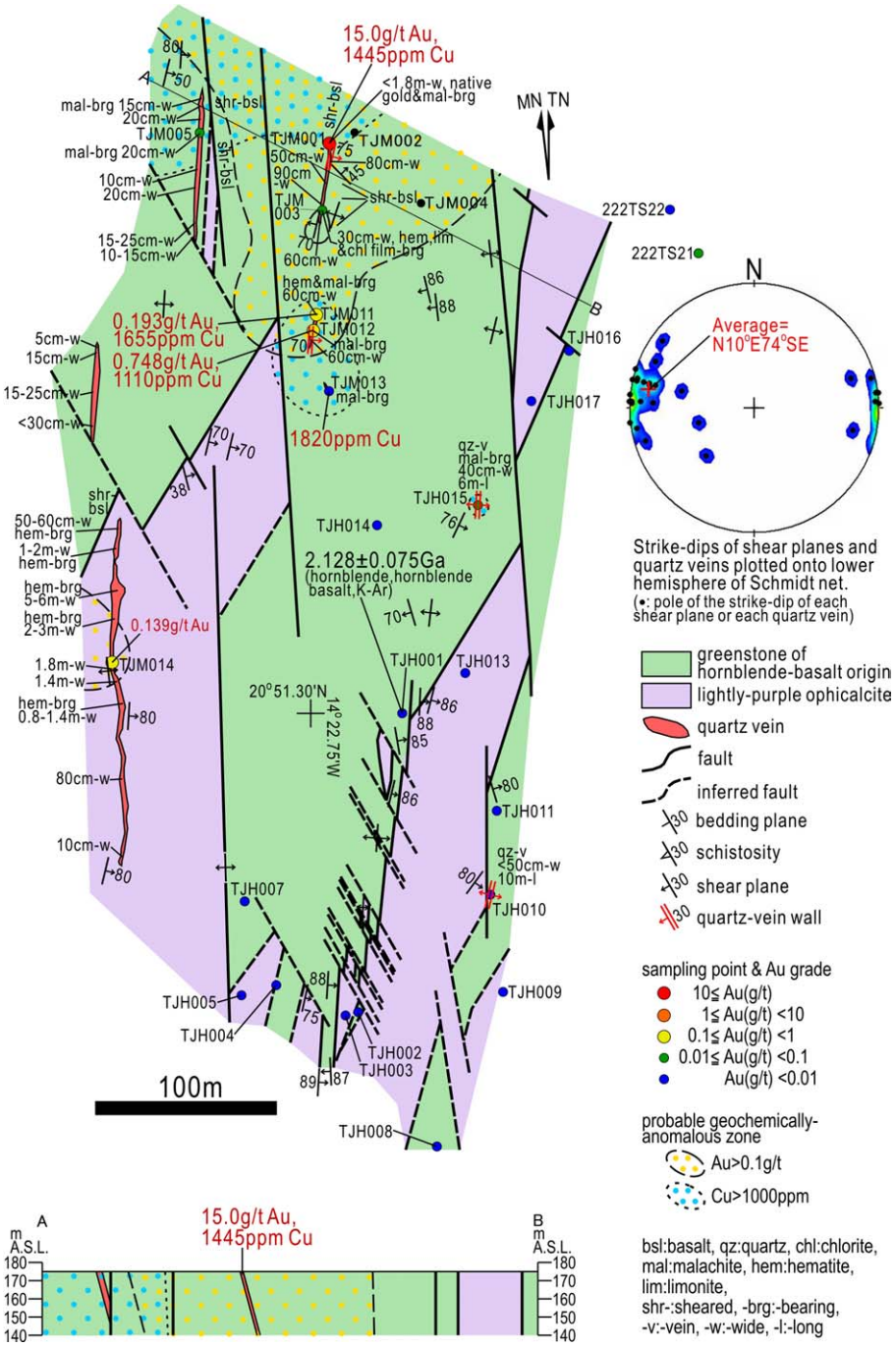

Fig. 4.3.11 Geological and geochemical maps of the Tijirit area

(5) Guelb Moghrein

(a) Geology

The northern part of the Akjoujt area consists of the Amsaga basement of the Archean,

while the eastern side contains layers of the Taoudeni Sedimentary Basin. The main geological unit in this area is the Akjoujt metabasalt (metadolerite, metabasaltic volcanics) of the Oumachoueima group consisting of calcareous schist, ferruginous quartzite, serpentinite, and so on. In the SW section of the area, the Hajar Dekhen granites thrust over the Oumachoueima group (Fig. 4.3.12).

Near the Guelb Moghrein deposit there is a widely distributed chlorite schist that has originated from (andesitic-) basaltic volcanic rocks, and also includes block- or lens-shaped carbonate bodies, and in some place there are outcrops of muscovite schist and black schist. The strike of the schistosity is either WNW-ESE or NW-SE, with a SW dip of 25-40°, which is in conformity with the overall area.

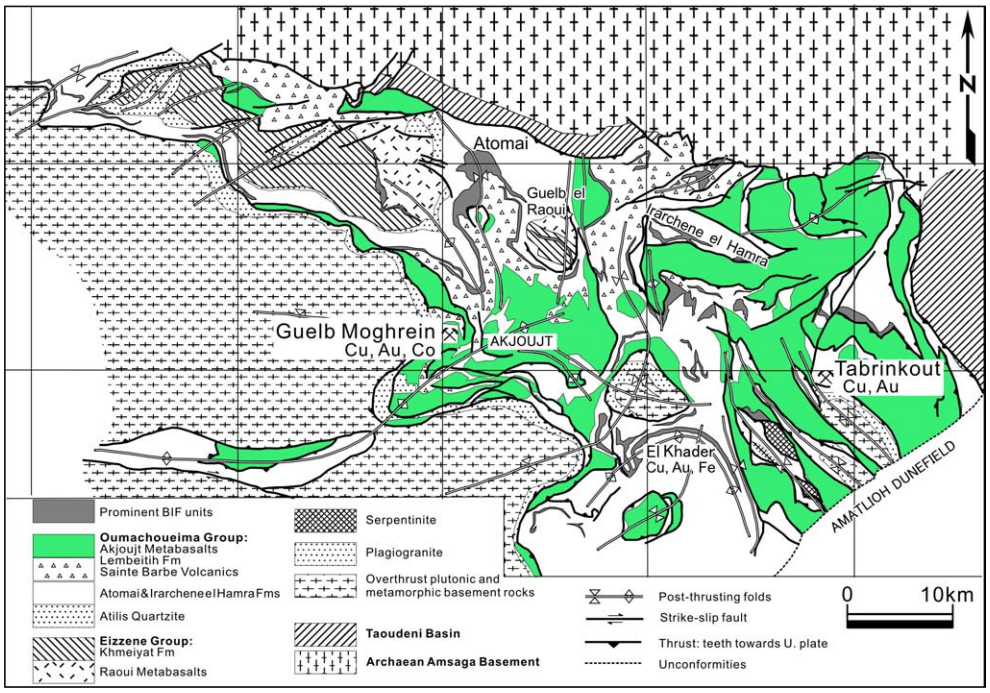

(modified Strickland and Martyn, 2001)

Fig. 4.3.12 Regional geological map of the Akjoujt area

(b) Deposit

The Guelb Moghrein Deposit is composed of a western ore body and an eastern ore body lying in harmony with the schistosity of the chlorite schist. Currently the excavation focuses on the western body only and has exposed its upper part. The ore body is 60m wide, 20m thick and more than 300m long and consists of carbonate rock replacement with lens-shaped magnetite-malachite ore bodies (Fig. 4.3.13). The strike is N 30-60° W, and the dip is 30-70° SW. The boundary between the carbonate rock and the chlorite schist is sharp. The schist directly below the ore body hosts occurrences of talc, anthophyllite and cummingtonite (Fig. 4.3.14). The carbonate rock is lumpy and contains large amounts of iron oxides (magnetite, hematite, and limonite) which are light brown to

reddish-brown in color. The carbonate rock consists of dolomite and magnesite, and is dominant in magnesium (Fig. 4.3.15).

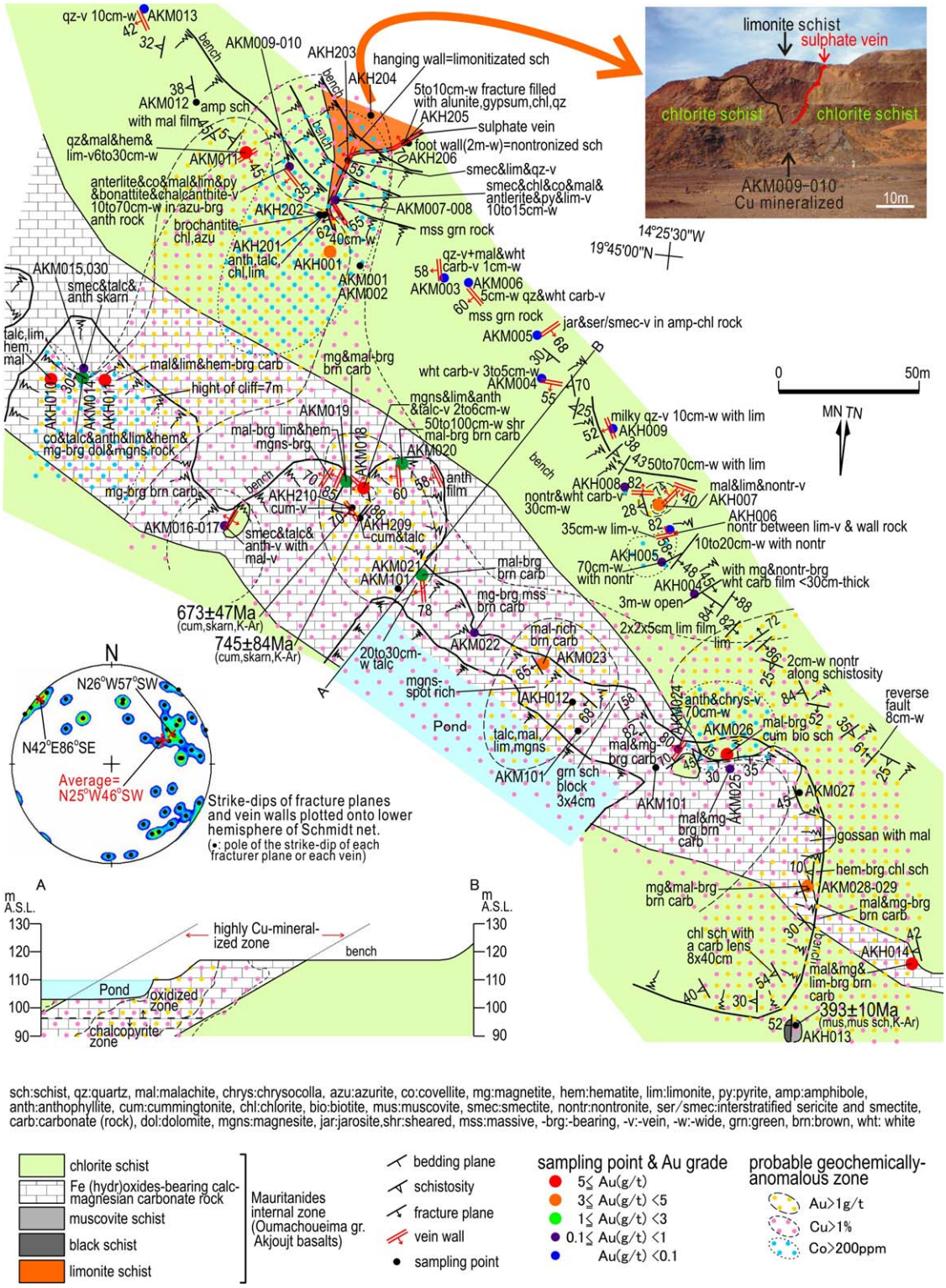

sch:schist, qz:quartz, mal:malachite, chrys:chrysocolla, azu:azurite, co:covellite, mg:magnetite, hem:hematite, lim:limonite, py:pyrite, amp:amphibole, anth:anthophyllite, cum:cummingtonite, chl:chlorite, bio:biotite, mus:muscovite, smec:smectite, nontr:nontronite, ser/smec:interstratified sericite and smectite, carb:carbonate (rock), dol:dolomite, mgns:magnesite, jar:jarosite,shr:sheared, mss:massive, -brg:-bearing, -v:-vein, -w:-wide, grn:green, brn:brown, wht: white

Fig. 4.3.13 Geological and geochemical maps of the Guelb Moghrein deposit

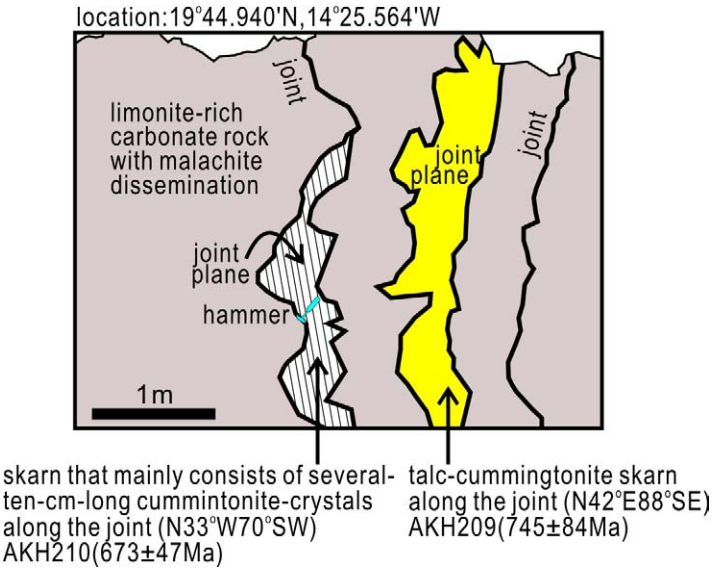

Fig. 4.3.14 Cummingtonite and talc in limonitized magnetite-bearing carbonate

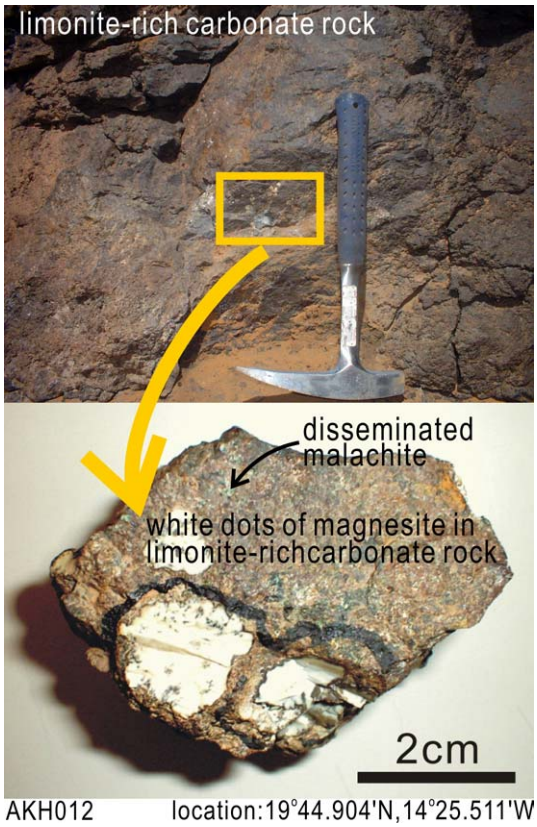

Fig. 4.3.15 Magnesite concentrate in limonitized magnetite-bearing carbonate

There are sulfate minerals (accompanied by covelline and malachite) that fill the 5-20cm-wide fissure that runs for about 20m through the chlorite schist of the footwall toward the top (Fig 4.3.16). On one section of the surface, 5-10cm-wide quartz veins have been observed that cut through the magnetite-bearing carbonate rock, or have formed roughly parallel to the schistose plane in the chlorite schist of the lower part of the deposit. These veins are often associated with malachite, nontronite, chlorite, and so on.

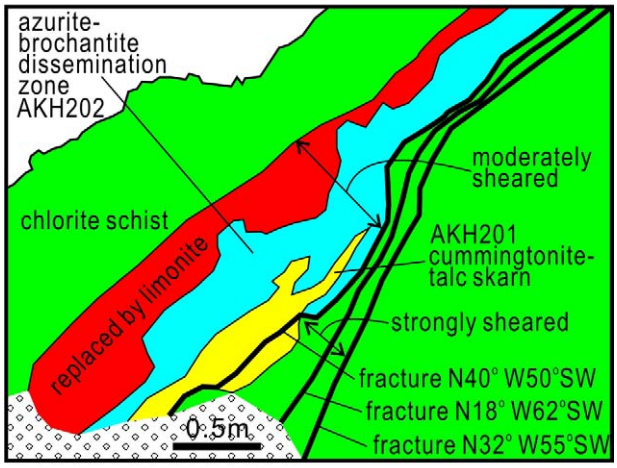

Fig. 4.3.16 Outcrop of fissure with sulfate minerals

Observation of the drill cores has confirmed primary sulfide minerals such as pyrite and pyrrhotite in the magnetite-containing carbonate rock and chlorite schist (Fig. 4.3.17).

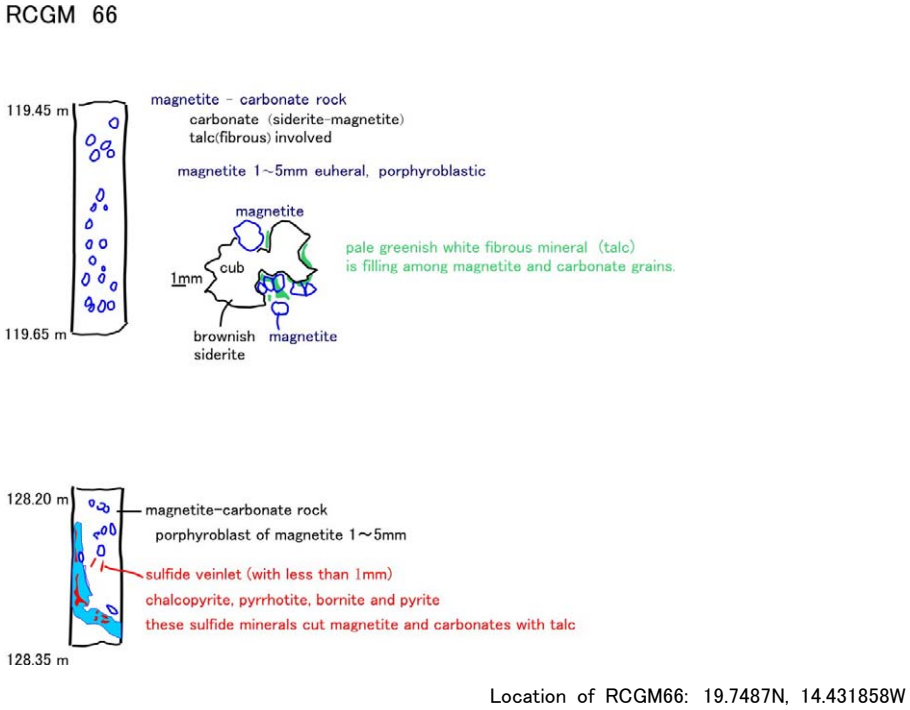

Fig. 4.3.17 Occurrence of mineralized part in drill core on the Guelb Moghrein (1)

The magnetite is euhedral with coarse grains of roughly 1mm in diameter. In the upper part of the ore body, malachite, crysocolla and azurite are concentrated along fissures in the carbonate rock or in a filmy or disseminated form.

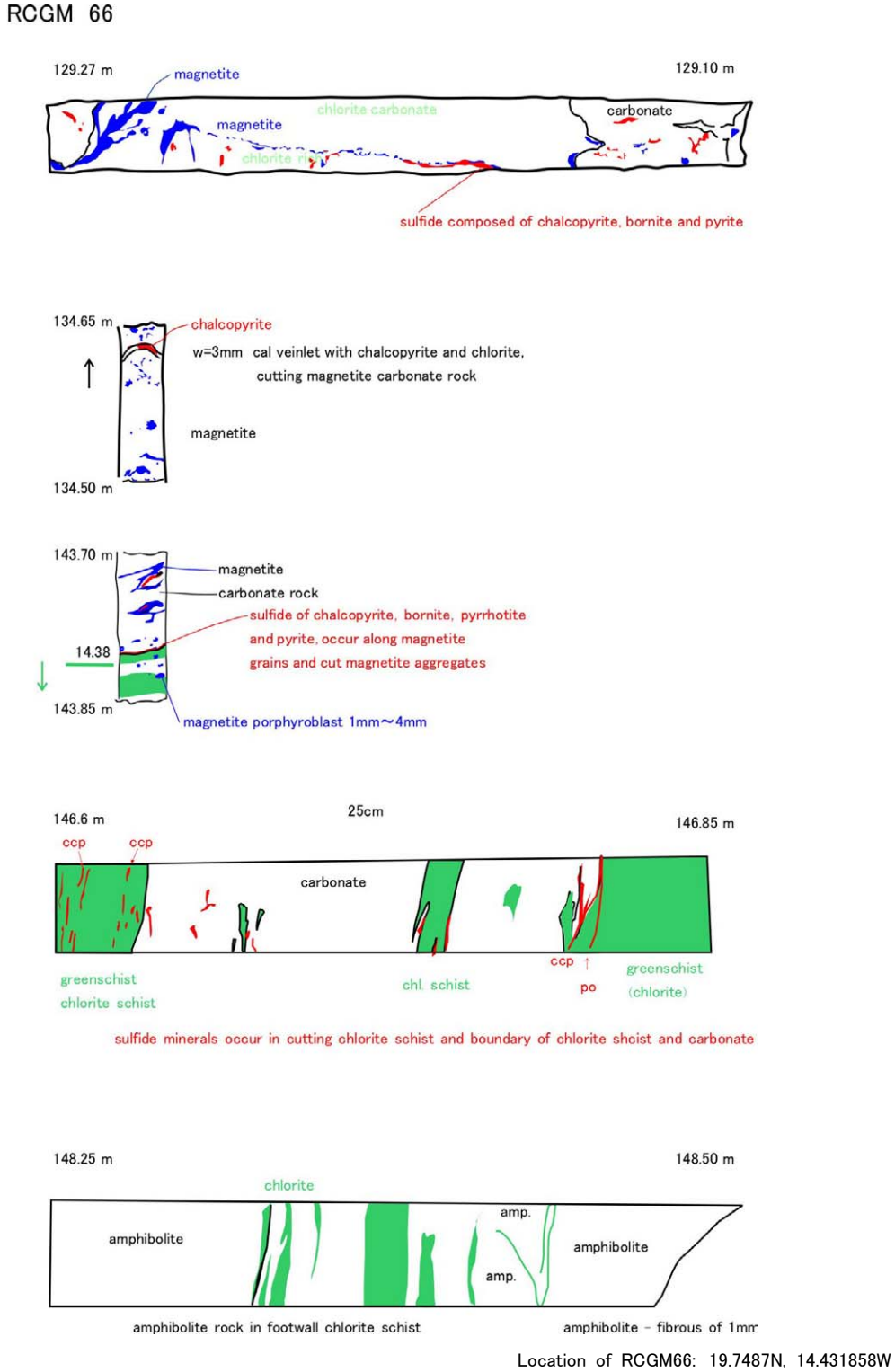

Fig. 4.3.17 Occurrence of mineralized part in drill core on the Guelb Moghrein (2)

(c) Results of Laboratory Work

[X-ray diffraction analysis]

X-ray diffraction analysis is presented in Appendix I-2.4. Carbonate is chiefly composed of magnesite associated with dolomite. Siderite has not been found. A part of the footwall schist of the carbonate ore body consists of nontronite, talc and anthophyllite. The mineral assemblages and chemical composition suggest the original rock of the ore deposit to be dolomite that is Mg predominant. Copper oxide ore comprises malachite, azurite, chysocolla and copper sulfosalts of antlerite, bonattite and chalcanthite.

[Chemical assay]

Descriptive statistics of 48 elements is shown in Appendix I of the Interim Report. The maximum Au is 9.89 g/t and 14 samples are represented over 1 g/t. Gold mineralization is recognized in many points. Native gold, however, is observed under the microscope only. Using the chemical assay method, a principal component analysis was conducted. In the second factor of the factor matrix, as elements show strong positive correlation with Au, the value of factor loading is more than 0.7, Ag, As, Bi, Co, Cu, Ge, In, Ni, Se, Sn, Te, and Zn (Appendix I of the Interim Report). Cr is extracted as a strong negative correlative element with Au.

The geochemical anomaly map representing gold, copper and cobalt anomalies (>1 ppm Au, > 1 % Cu and > 200 ppm Co) was drawn and overlapped with geological map of Fig.4.3.13. Copper anomaly over 1% covers the distribution area of carbonate ore. Gold anomaly over 1 ppm overlaps copper anomaly, and parts of gold anomaly also exist in green schist. Cobalt anomaly over 200 ppm is distributed in the green schist of the footwall.

[Fluid inclusion test]

Fluid inclusions are observed in quartz crystal of the quartz veins accompanied by malachite and limonite, cutting the footwall green schist. The size of the fluid inclusions ranges from 10 to 20 micrometers. Fluid inclusions are dominantly composed of polyphase inclusions containing halite crystals, with gaseous inclusions. The homogenization temperature ranges between 240 and 320°C, and salinity varies from 33 to 39 wt% NaCl eq. (Appendix I of the Interim Report).

[Dating]

K-Ar dating of cummingtonite in magnesian carbonate from the ore deposit shows 745±84Ma and 673±47Ma (Appendix I of the Interim Report). It corresponds to Strutian period of the Proterozoic. This time suggests the deposit formation age.

(d) Consideration

It is suggested that the deposits were formed after the replacement of carbonate rock by ore solution, because copper and gold mineralization occurs restrictedly in and around magnesium-rich magnesitic and dolomitic carbonate rocks in the green schists. Thus, the ore body shows lenticular form owing to the reflection of occurrence of original rock.

In the lower part of the carbonate ore body, magnetite is accompanied by sulfide minerals of pyrite, chalcopyrite and covellite. On the other hand, the upper part of the ore body shows development of an oxide zone, which comprises iron oxide, copper carbonates and copper sulfosalts composed of goethite, malachite, azurite, chysocolla, antlerite, bonattite and chalcanthite. This suggests that the copper found in the upper part of the ore body having been oxidized by oxygen, afterwards dissolved in the shallow meteoric groundwater.

By the naked eye gold concentrates can be seen to be associated with copper oxides composed of malachite, azurite and chysocolla. It is also clear that the gold geochemical anomaly overlaps with the copper anomaly. The above facts allow assuming that gold and copper acted similarly in the process of transformation from ore fluid to their precipitation.

Concentrations of copper and gold mineralization are disseminated and found in veins along fractures and fissures in the Guelb Moghrein deposit. Thus, it shows that the fracture zone and fissures formed by the results of tectonic movement in the host rock had become main pathways of the hydrothermal solution.

The quartz veins cutting magnetite-bearing carbonate rocks, those with gold-bearing copper minerals running parallel to schistosity, are the evidence of the pathways of hydrothermal activities from the depth. In the quartz veins with malachite, polyphase inclusions containing halite crystals are generally observed. Homogenization temperature ranges from 240 to 320ºC, and salinity reaches 33-39 wt% NaCl eq. Thus it suggests that high saline fluid is related to copper and gold mineralization. Because cobalt and nickel are the dominant elements in mafic rocks, both elements could have been transported from the below rocks of the carbonate and mafic rocks around the deposit. The decrease in chromium implies that the ore-forming fluid had oxidized chromium in the mafic and ultramafic rocks and dissolved it.

Peculiarity of gold mineralization in the Guelb Moghrein deposit suggests the Au, Cu, Co, Ni, Zn, Ag, As elements had precipitated with strong positive correlation mutually showing in the loading factor of a principal component analysis. Cobalt and nickel could have been transported from around the mafic rocks as described above. It is possible that gold, silver, copper and arsenic be associated with acidic plutonic rocks under the intermediate or acidic near intermediate circumstance rather than mafic rocks (e.g. Thompson and Newlerry, 2000; Sato, 2000).

[Remote sensing analysis]

ASTER image of the Akjoujt area including the Guelb Moghrein and Tabrinkout, and ASTER images of the vicinity of the Guelb Moghrein deposit are shown in Fig 4.3.18. The assessment of image analysis is as follows:

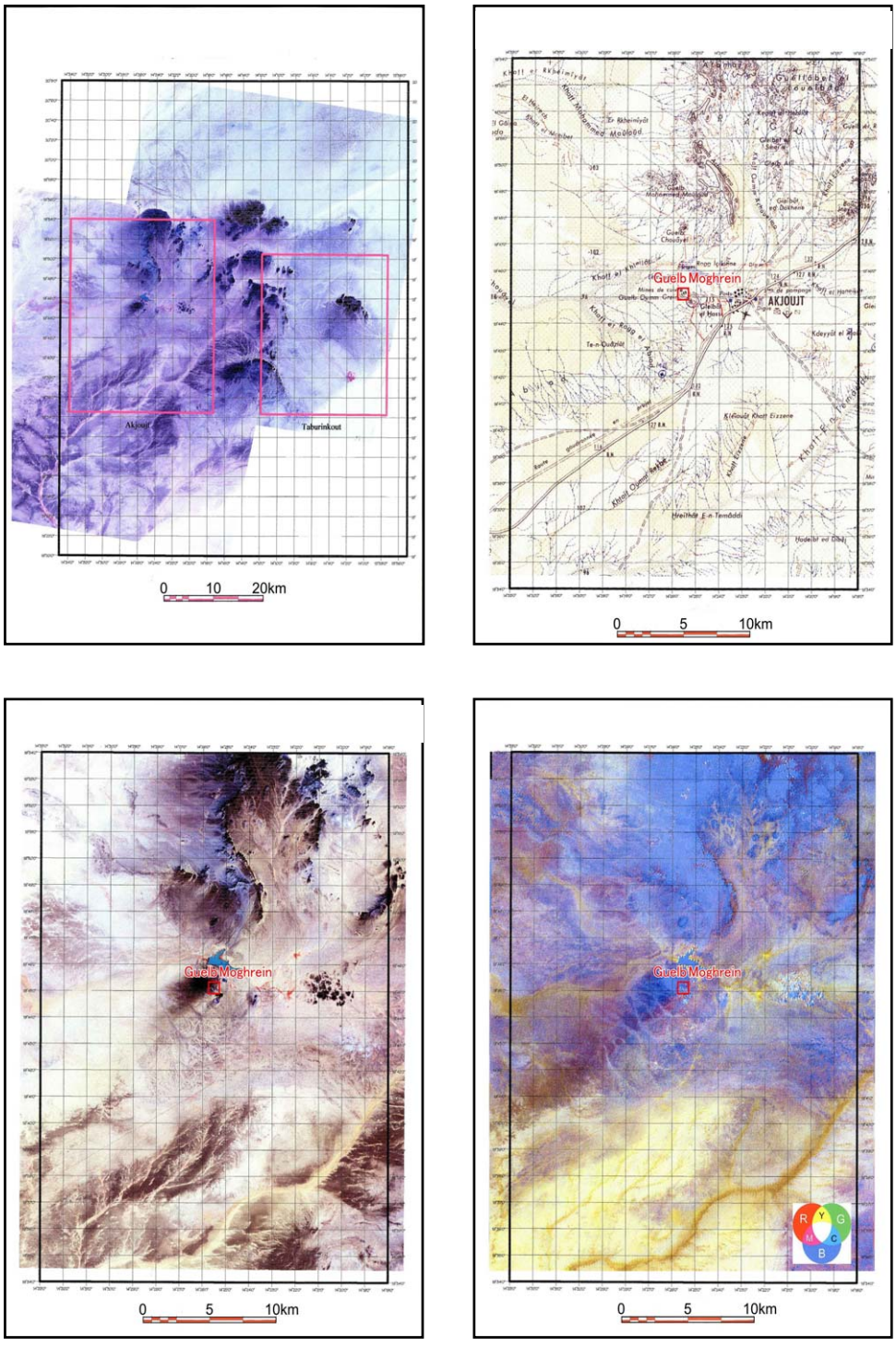

Fig. 4.3.18 Satellite images of the Akjoujt area and the Guelb Moghrein deposit

- Akjoujt metabasalt containing carbonate rocks and silicified gossans where the Guelb

Moghrein deposit is formed is distinguished in coarse texture and brown lothofacies on the ASTER False color image.

- In the southern and southeastern part of the Guelb Moghrein deposit, the Akjoujt metabasalt is extracted in blue (iron oxide) or bluish green mixed with reddish purple (iron oxide and carbonate) on the band rationing (RGB: 4/8, 4/9, 1/3). This rationing is effective to select the Akjoujt metabasalt.
- But, in the northern part of the deposit, blue on the rationing image distributes widely, and the Amsaga basement (granite and migmatite) is even included in an area of the blue color.

(6) Guidimaka

There are five chromite deposits in the surveyed area (BRGM, 1975). The present geological survey has focused on the No.1, No.2 and No.3 deposits among them (Fig. 4.3.19). BRGM implemented pitting and trenching there in 1974 and found three major deposits. These ore orebodies are 55m x 3m in scale at the northern lens, 10m x 1m at the central lens and 15m x 3m at the southern lens. The ore reserves were estimated to be 700 to 900 tons per meter of down-dip extension. The average grade is 25.5 % Cr_2O_3 (BRGM, 1975).

The No.1 deposit is located about 5 km east of the Diaguili village and is situated on the northwestern part of the hill which trends N-S with about 40m asl. The north-trending hill consists of siliceous pelitic schist, and serpentinite and chlorite schist occur in the northwestern part of the hill. The pelitic schist strikes N10-20°E and dips 40-60° west. The pelitic schist includes layers of iron-oxide with siliceous part.

Serpentinite exposes in an area of about 200m width in east-west and about 500m extension in north-south (Fig. 4.3.20). Serpentinite intercalates layers of chlorite schist with 10m to 20m thickness, Schistosity of schistose serpentinite and chlorite schist strikes NE-SW and dips 60-65 ° southeast or 40-70 ° northwest. Based on the schistosity, the unit composed of serpentinite and chlorite schist has probably anticline with an axis of NE-SW direction.

The serpentinite consists of monotonous serpentine with chromite of about 1mm in size. Observation under the microscope shows that it is composed of serpentine replaced olivine and pyroxene, and veinlet of serpentine. Chromite is anhedral and 0.5mm to 1mm in size, and altered to magnetite and hematite in the rim of grain (AppendixI-2.6). Lizardite and chysotile are identified by X-ray analysis (AppendixI-2.7). Chlorite schist consists mainly of chlorite, and a little amount of ilmenite and magnetite observed under the microscope (Appendix I-2.7).

Six chromite orebodies in the serpentinite unit are exposed on the surface. They are 10m to 40m long and a few meters to 15m thick. Chromite ores are massive, and consist of coarse-grained chromite. Blind chromite orebodies could be buried under the surface. The orebodies are of podiform type.

The No.2 deposit is located about 4 km north-northeast of the Diaguili village. The deposit is 90m x 70m in scale. Since serpentinite lies about 350m southeast far from the chromite orebody, the direct relation between chromite and serpentinite on the surface (Fig. 4.3.21). The No.3 deposit crops out 4m x 5m in a small scale locating 2km northeast of the No.1 deposit, and situating westward of serpentinite body trending N-S (Fig. 4.3.22).

Chromite ore at each outcrop is assumed Cr2O3 grade of 30%, and there is no difference of grade at outcrops respectively. Chromite and magnetite disseminate as around 1mm grain in serpentinite.

Microscope observation shows massive chromite ore to be composed of chromite, magnetite, chlorite and serpentinite. Chromite is transparent brown to yellowish brown, and 0.3mm to 5mm in size. Numerous fractures run in the chromite ore, and along the fractures it changes to opaque and partly altered to magnetite.

The chromite grains are analyzed by X-ray Diffraction analyzer and Energy Dispersive X-ray spectrometer (EDX). It is confirmed that most of grains is ferro-magnesiochromite $(Fe,Mg)((Cr,Al)_2O_4)$ that is solid solution of chromite, and little of grains is chromite (Appendix I-2.3 and I-2.8). Ferro-magnesiochromite is massive and runs numerous cracks. It is brownish red to yellowish brown in transparent light, and is sometimes opaque. Untenbogaardt and Burke (1985) describe that zonal texture is common, and this is due to differences in chemical composition. Usually the core is richer in Mg and Al and the marginal zones have a higher Fe and Cr content. Chromite in this deposit occurs around magnesiochromite grains and along the cracks of them. It is assumed that chromite and magnesiochromite are formed due to differences in chemical composition from their occurrence, that and two minerals shows zonal texture. Metal contents of ferro-magnesiochromite in the Guidimaka deposit represent 35.0−45.6% Cr, 17.7-33.8% Fe, 2.3-8.9% Mg and 2.0-15.5% Al, due to semi-quantitative analysis of EDX. Transparent foliated chlorite, acicular and foliated serpentine occurs among chromite grains and cracks of ferro-magnesiochromite (Appendix I-2.3).

In general the content of commercial chromite ore ranges from 35 to 55% Cr_2O_3. The chromite ores are classified into three grades based on their content of Cr_2O_3 (Table 4.3.1). Based on the present survey, the grade of the chromite ores in the Guidimaka is low, and varies from 22.6 to 33.7% Cr_2O_3 (Appendix I-2.8). The low grade ores in this deposit are caused by chemical composition of chromium minerals that are chiefly magnesiochromite, and not chromite. Only a little amount of the chromite ores is applied for the refractory use.

Table 4.3.1 Classification of chromite ore

Purpose	Cr_2O_3 (%)
Metallurgical grade	> 48%
Chemical grade	> 44%
Refractory grade	> 31%

(Reference: Yoshida, 1992)

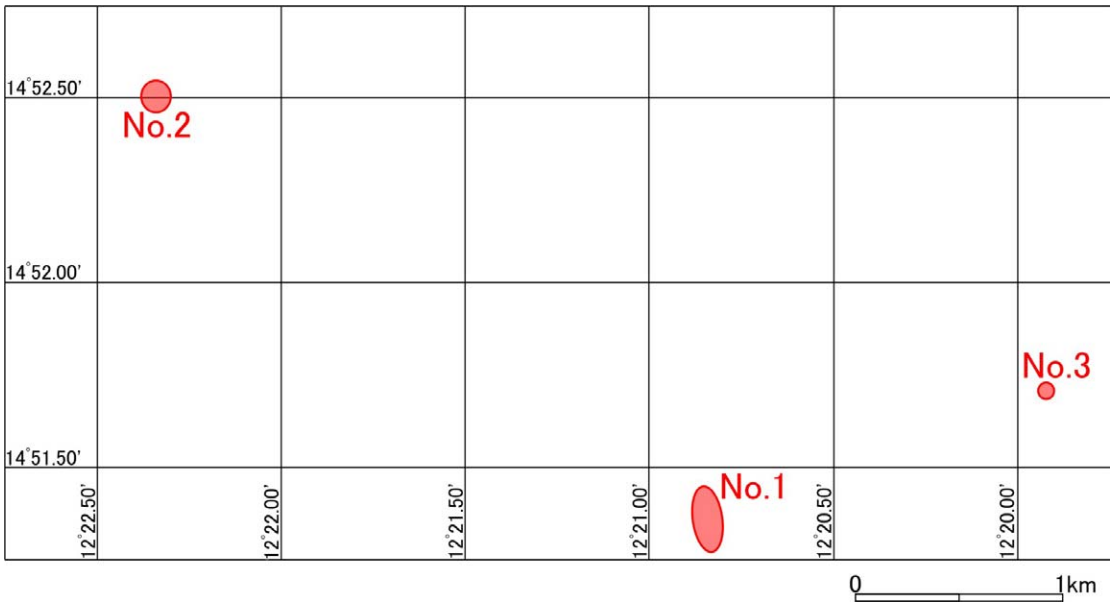

Fig. 4.3.19 Location of the Guidimaka deposit

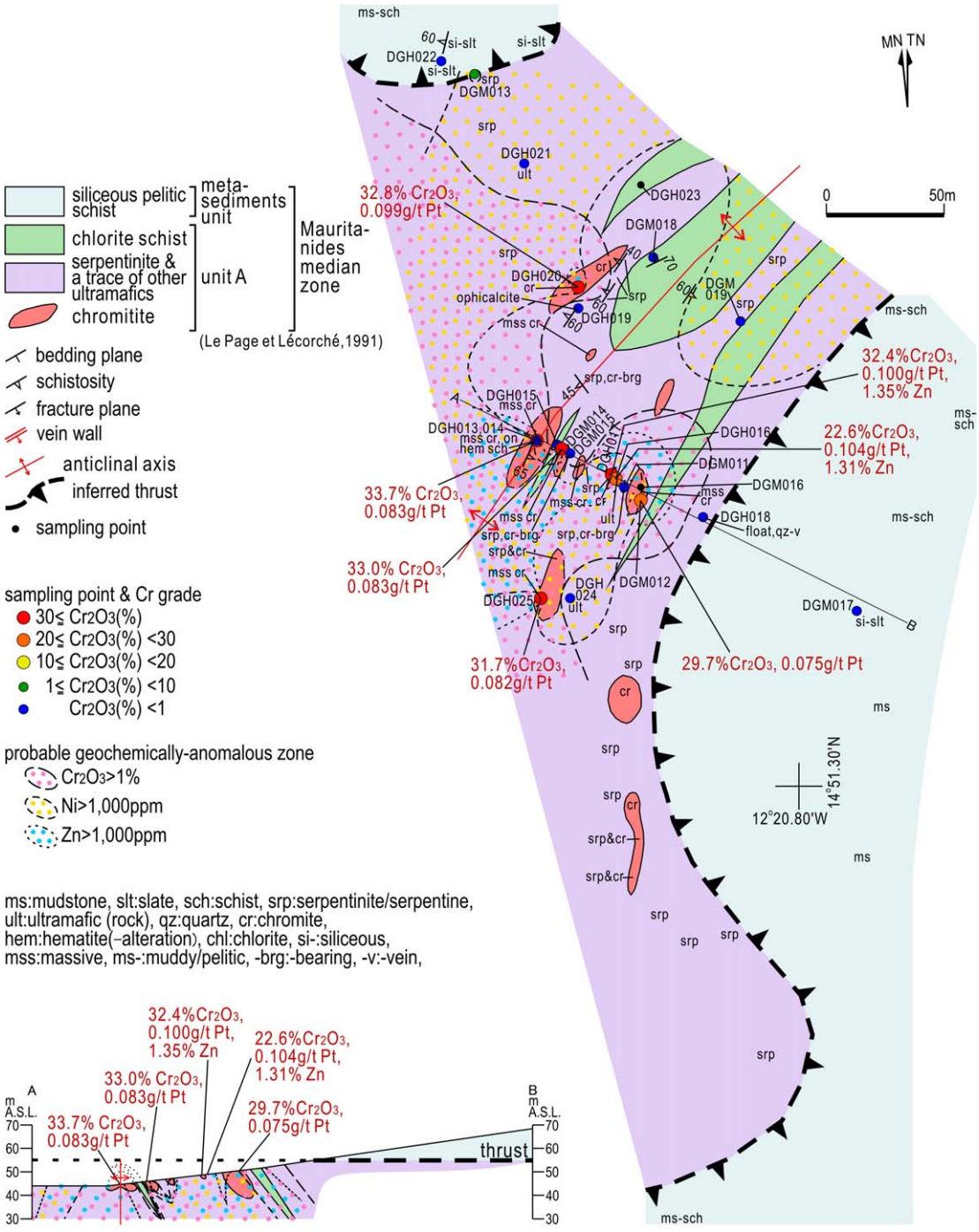

Sample	stoichiometry of chromite (total cation=3)								Pt(g/t)
	Al	Cr	Fe(Ⅲ)	Fe(Ⅱ)	Mg	Mn	Ni	Zn	
DGH017	0.758	1.027	0.216	0.204	0.641	0.099	0.006	0.050	0.100
DGH020	0.800	1.066	0.134	0.202	0.728	0.059	0.005	0.006	0.099
DGH013	0.856	1.036	0.108	0.251	0.684	0.054	0.004	0.006	0.083
DGM014	0.829	1.029	0.141	0.210	0.700	0.065	0.005	0.019	0.083
DGH025	0.765	1.006	0.228	0.180	0.729	0.082	0.004	0.005	0.082
DGM012	0.723	0.967	0.310	0.101	0.774	0.102	0.004	0.018	0.075
DGM016	0.793	0.998	0.209	0.135	0.780	0.071	0.004	0.009	<0.005
correlation with Pt	−0.011	0.469	−0.205	0.516	−0.663	0.084	0.426	0.304	
2−tailed sig.	0.982	0.288	0.659	0.236	0.104	0.858	0.341	0.507	

Fig. 4.3.20 Geological and geochemical maps of the Guidimaka No.1 deposit

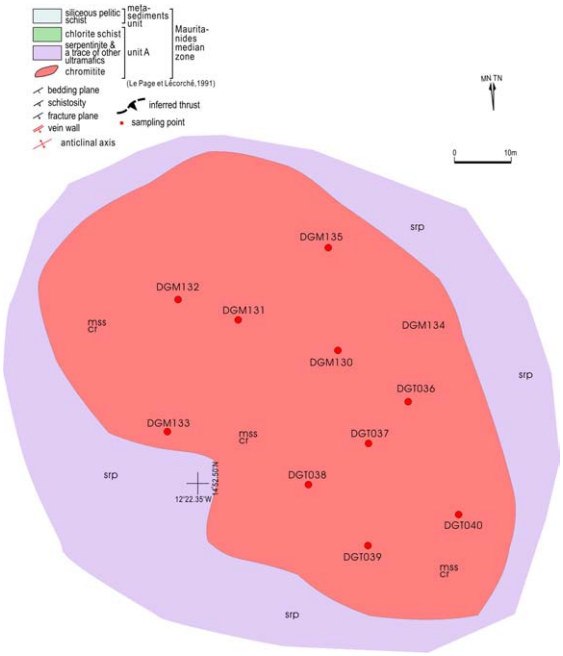

Fig.4.3.21 Geological map of the GuidimakaNo.2 deposit

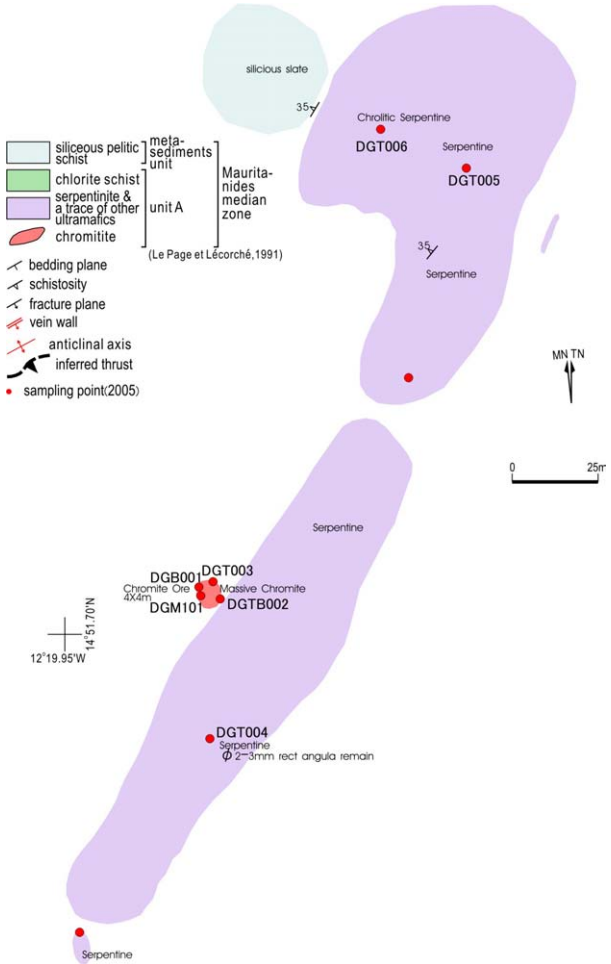

Fig.3.22 Geological map of the GuidimakaNo.3 deposit

The chromite ores in the Guidimaka deposit have revealed the grade of 0.07 to 0.104 g/t Pt in this survey (Appendix I-2.5). Ore minerals except ferro-magnesiochromite and chromite are observed in the polished thin section showing high platinum content. The following five kinds of platinum group minerals (PGM) are confirmed by semi-quantitative analysis of EDX and qualitative analysis of EPMA (Electron Probe Micro-analyzer) (Appendix I-2.8 and I-2.3).

Osmium: Os, Irarsite: (Ir,Ru)AsS, Laurite: RuS_2, Erlichmanite: OsS_2, Cuproiridsite: $CuIr_2S_4$

Osmium, Erlichmanite and Cuproiridsite occur as grains of 0.003-0.005mm in size in ferro-magnesiochromite. Irarsite and Laurite form as grains of 0.002-0.007mm in size in chlorite filled ferro-magnesiochromite grains.

Chalcopyrite, galena and nickel sulfide minerals as pentlandite and millerite are occur as other sulfide minerals except PGM (Appendix I-2.8 and I-2.3).

Laboratory works shows that platinum group elements detected in the Guidimaka deposit are osmium, iridium and ruthenium, and PGM forms as metal grains or sulfide grains coexisting with ferro-magnesiochromite. PGE analyzed in this investigation are platinum and palladium. It is recommended that osmium, iridium and ruthenium are analyzed in future.

[Remote sensing analysis]

LANDSAT image of the Selibaby area including the Guidimaka, Diaguili and Oudelemguil, and ASTER images of the vicinity of the Guidimaka deposit are shown in Fig 4.3.23. The assessment of the image analysis is as follows:

- The units of serpentinite where the chromite orebodies in the Guidimaka deposit lie, are distinguished from other lothofacies because they form hills with grayish green tint geographically on the ASTER False color image.
- ASTER Band Ratio image is not fit for the discernment of serpentinite because the entire image become dark blue. In ASTER HIS processed image (HIS: 8, 7,4) presented in right bottom of Fig. 4.3.23, drainage pattern, agriculture farm and hills except barren land are pale brown, and this rationing process is not suitable for the extraction of the serpentinite.

It is clarified that the ASTER False color image is better than the processing images such as Band Ration and HIS, for the extraction of the serpentinite in the Guidimaka area.

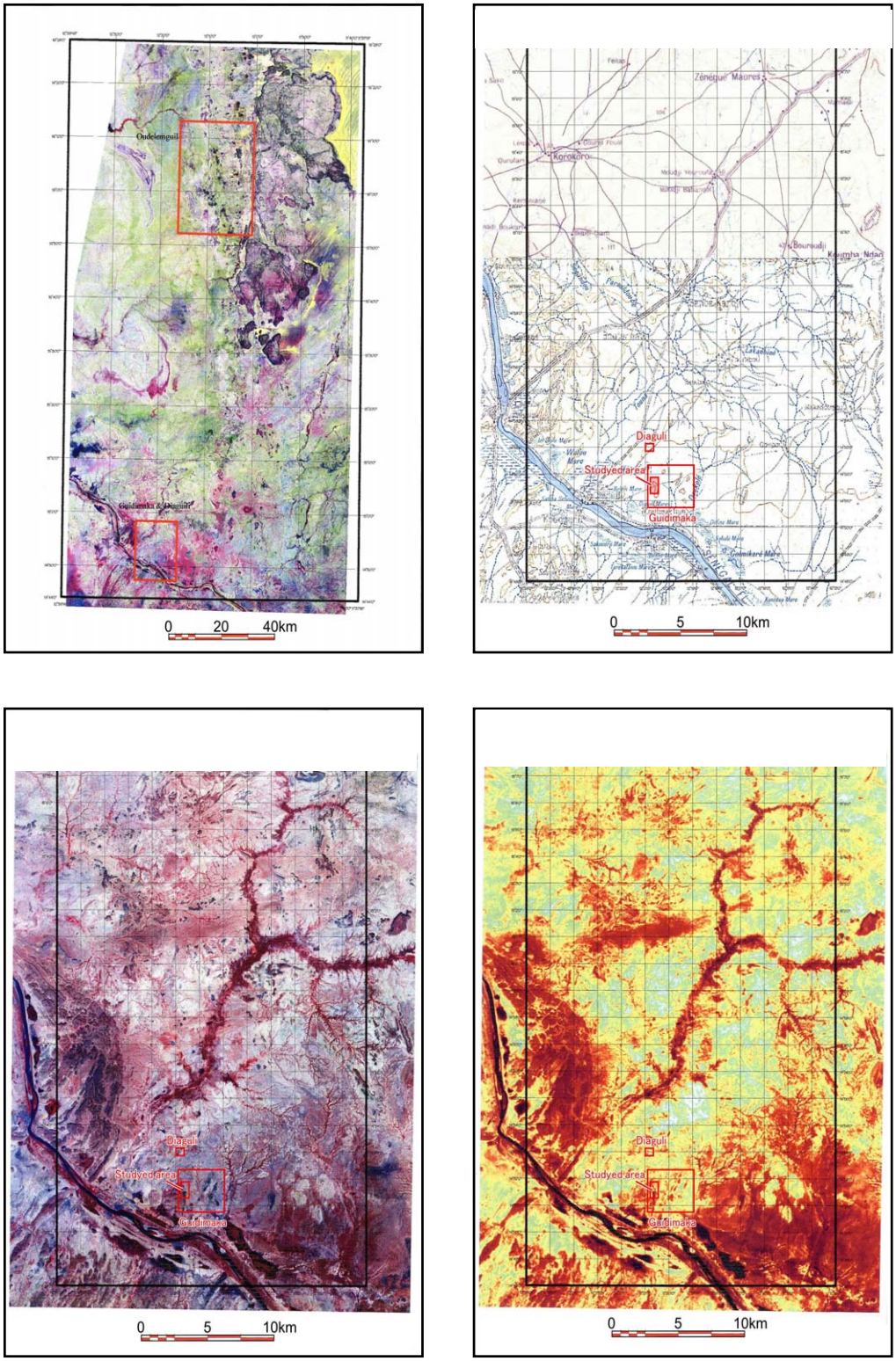

Fig. 4.3.23 Satellite images of the Selibaby area and the Guidimaka deposit